

## Experimental Observation of a Strange Nonchaotic Attractor

W. L. Ditto, M. L. Spano, H. T. Savage, S. N. Rauseo, J. Heagy, and E. Ott<sup>(a)</sup>

Naval Surface Warfare Center, Silver Spring, Maryland 20903-5000

(Received 22 March 1990)

Evidence is presented for the existence of a strange nonchaotic attractor in a two-frequency quasi-periodically driven, buckled, magnetoelastic ribbon experiment. Scaling behavior in the Fourier amplitude spectrum is observed in agreement with predicted scaling behavior for strange nonchaotic attractors. Dimension measurements also support the existence of a strange nonchaotic attractor.

PACS numbers: 05.45.+b, 75.80.+q

Recently, much attention has been given to dissipative dynamical systems with quasiperiodic driving terms. These systems are a natural extension of periodically forced systems, but offer richer dynamical possibilities. In a recent series of papers<sup>1-5</sup> it was shown that two-frequency quasiperiodically forced systems can exhibit a new class of dynamical behavior which the authors term *strange nonchaotic*. In this instance the word *strange* refers to the geometry of the underlying attractor as exhibiting a fractal structure, while the word *nonchaotic* refers to the particular dynamics of orbits on the attractor. A chaotic attractor is an attractor for which nearby orbits diverge exponentially in time, displaying sensitive dependence on initial conditions (at least one positive Lyapunov exponent). A nonchaotic attractor, however, is an attractor for which nearby orbits typically do not diverge exponentially in time (no positive Lyapunov exponents). Consequently, a strange nonchaotic attractor is an attractor that is geometrically strange, but for which nearby trajectories do not diverge exponentially.

It has been shown that strange nonchaotic attractors are typical in quasiperiodically forced systems.<sup>3</sup> Here, typical means that the attractors exist over sets of positive measure in parameter space. Thus precise parameter tuning is not necessary in order to observe these attractors in experiments. In a previous Letter<sup>2</sup> it was shown that transitions between two-frequency quasiperiodicity and strange nonchaotic behavior in a damped, quasiperiodically driven pendulum equation can be associated with transitions from stop band to (Anderson) localized solutions of the Schrödinger equation with a quasiperiodic potential. While there are reports of the transition to *chaotic* behavior in experimental systems that are quasiperiodically forced,<sup>6-8</sup> the identification of a strange nonchaotic attractor in an experimental system has not been reported. In this paper we present the first report of a strange nonchaotic attractor in an experiment and the first verification of the predicted power-law scaling of spectral components for such an attractor.

In order to identify strange nonchaotic attractors in experiments, we need to identify the potentially measurable signatures that characterize these attractors. In particular, we discuss below the Fourier amplitude spec-

tra of time series, Lyapunov exponents, and fractal dimensions.

**Fourier amplitude spectra.**—The discrete-time Fourier amplitude spectrum  $|S(f)|$  as a function of frequency  $f$  for a time-varying quantity is the magnitude of the Fourier transform of the discrete-time series obtained by sampling the quantity at one of the two driven frequencies of the quasiperiodic forcing. In practice any  $\delta$  functions contained in  $|S(f)|$  acquire a width and a finite peak value (e.g., due to the finite duration of the time series). A peak is defined as a local maximum in the discrete spectrum. Define the *spectral distribution function*  $N(\sigma)$  as the number of peaks  $|S(f)|$  with amplitude greater than  $\sigma$ . Distinct scaling relations for  $N(\sigma)$  have been predicted for two-frequency quasiperiodic attractors, three-frequency quasiperiodic attractors, and strange nonchaotic attractors. These relations are respectively<sup>2-4</sup>  $N(\sigma) \sim \ln(\sigma)$ ,  $N(\sigma) \sim [\ln(\sigma)]^2$ , and  $N(\sigma) \sim \sigma^{-\alpha}$ ,  $1 < \alpha < 2$ .

**Lyapunov exponents.**—In the case of two-frequency quasiperiodic forcing there are two Lyapunov exponents that are trivial in the sense that they are identically zero by virtue of the two forcing frequencies. Let the Lyapunov exponents  $\lambda_i$  be ordered by size,  $\lambda_1 \geq \lambda_2 \geq \lambda_3 \geq \dots$ . We then have the following possibilities: (1) two-frequency quasiperiodic attractors,  $\lambda_1 = \lambda_2 = 0 > \lambda_3$ ; (2) three-frequency quasiperiodic attractors,  $\lambda_1 = \lambda_2 = \lambda_3 = 0 > \lambda_4$ ; (3) chaotic attractors,  $\lambda_1 > 0$ ; and (4) strange nonchaotic attractors, the same as two-frequency quasiperiodic attractors. For our system we were unable to obtain reliable results for the nontrivial Lyapunov exponents (except for  $\lambda_1$  in the chaotic case) by direct application of standard techniques (since the exponents would all be negative).<sup>9</sup> Nevertheless, reliable indirect evidence is available from measurements of the information dimension.

**Dimension.**—The information dimension of an attractor is defined as  $d_i = \lim_{\epsilon \rightarrow 0} [I(\epsilon)/\ln(1/\epsilon)]$ , where the attractor has been covered by cubes from a Cartesian grid of spacing  $\epsilon$  in the phase space. Here  $I(\epsilon) = -\sum_{i=1}^{N(\epsilon)} p_i \ln(p_i)$ , where  $p_i$  is the measure of the attractor in the  $i$ th cube of the cover. In experiments  $p_i$  can be estimated as the fraction of time that a finite-

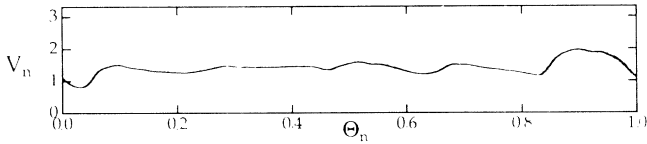


FIG. 1. Surface of section of output voltages  $V_n = V(t_n)$  vs  $(nf_2/f_1) \pmod{1}$  for  $H_1 = 0.71$  Oe and  $H_2 = 0.53$  Oe.

duration orbit spends in cube  $i$ . The presence of two-frequency quasiperiodic forcing guarantees that any attractor will be at least two dimensional. If the attractor is chaotic there is at least one unstable direction and the dimension should hence be at least three. Thus, if we calculate the information dimension and it is less than three ( $d_i < 3$ ) the attractor is nonchaotic. If the Kaplan-Yorke conjecture (which gives the information dimension in terms of the Lyapunov exponents<sup>10,11</sup>) applies for our strange nonchaotic attractor, then  $d_i = 2$ . (Note that  $d_i = 2$  does not rule out fractal structure. In particular, it has been claimed<sup>5</sup> that the capacity dimension  $d_c$  is strictly greater than the information dimension for strange nonchaotic attractors.)

Combining spectral-distribution scaling and dimension measurements one can systematically support or rule out the existence of each of the four above-mentioned attractors in an experimental time series for a two-frequency quasiperiodically forced system. In practice the dimension measurements are performed on surface-of-section data, reducing all of the dimensions discussed in the previous paragraph by one. We use a tilde to denote the dimension in the surface of section.

To summarize, the information we will be using is as follows. Two- (three-) frequency quasiperiodicity gives  $\tilde{d}_i = 1$  ( $\tilde{d}_i = 2$ ) with  $N(\sigma) \sim \ln(\sigma)$  ( $N(\sigma) \sim [\ln(\sigma)]^2$ ). A strange chaotic attractor occurs only if  $\tilde{d}_i \geq 2$ , and a strange nonchaotic attractor occurs if  $\tilde{d}_i < 2$  with  $N(\sigma) \sim \sigma^{-\alpha}$ .

The experimental system consisted of a gravitationally buckled, amorphous magnetoelastic ribbon. The ribbon material belongs to a new class of amorphous magnetostrictive materials that have been found to exhibit very large reversible changes of Young's modulus  $E(H)$  with the application of small magnetic fields.<sup>12,13</sup> The ribbon was clamped at the base to yield a free vertical length greater than the Euler buckling length, thus giving an initially buckled configuration. The ribbon was driven with a vertical magnetic field having the form  $H = H_1 \cos(2\pi f_1 t) + H_2 \cos(2\pi f_2 t)$ . The magnetic-field amplitudes were typically set in the range 0.50–0.90 Oe after compensating for the Earth's magnetic field. A sensor measured the curvature of the ribbon near its base. Other details of the experimental system can be found in Refs. 12 and 13.

The data were time series of voltages  $V(t)$  acquired from the output of the sensor. Voltages were sampled at the drive period of the  $H_1$  signal (times  $t_n = n/f_1$ ) by

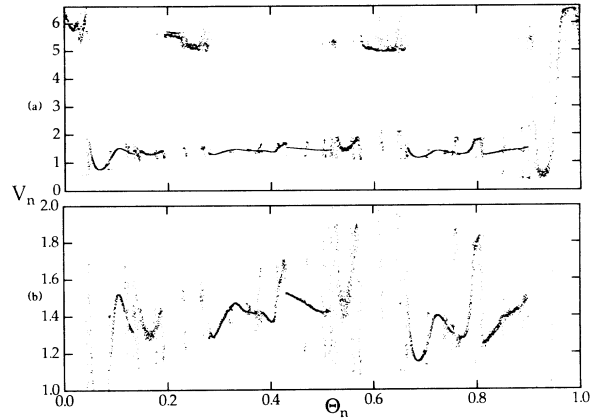


FIG. 2. (a) Surface of section of output voltages  $V_n = V(t_n)$  vs  $(nf_2/f_1) \pmod{1}$  for  $H_2 = 0.80$  Oe (5000 data points). (b) Same plot on different voltage scale indicating structure on several length scales.

triggering off the synthesizer producing the  $H_1$  signal. Time-one map data were obtained for approximately 3 h (5000 points) after discarding the initial 1 h of data to allow the ribbon motion to settle onto an attractor. Parameters were set at  $H_1 = 0.71$  Oe,  $f_1 = 0.5$  Hz,  $f_2 = \gamma f_1$ , where  $\gamma = (\sqrt{5} - 1)/2$  is the inverse of the golden mean, and  $H_2$  was varied as our control parameter. Inherent timing and drift problems were found to be insignificant for data runs of up to 4 h.

Surfaces of section were constructed by plotting output voltages  $V_n \equiv V(t_n)$  vs  $\theta_n \equiv (nf_2/f_1) \pmod{1}$ . For  $H_2 = 0.53$  Oe we found (Fig. 1) the attracting orbit in the surface of section to lie on a smooth curve, indicating quasiperiodic motion on a two torus. For  $H_2 = 0.80$  Oe the attracting set shows a fine-scale structure as can be seen on several length scales [Figs. 2(a) and 2(b)]. We present evidence below that this is a strange nonchaotic attractor.

In Fig. 3 we have plotted the Fourier amplitude spec-

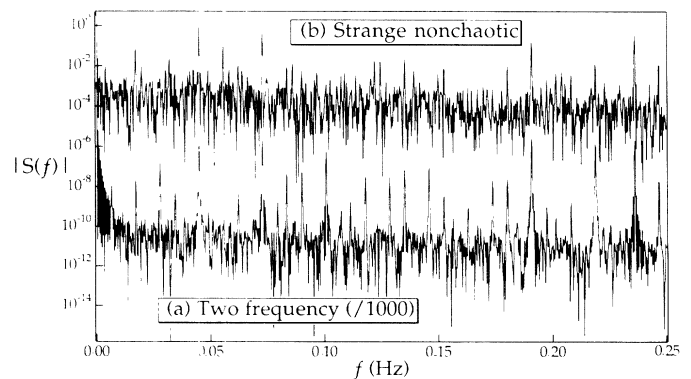


FIG. 3. Fourier amplitude spectra  $|S(f)|$  of output voltages  $V_n$  vs frequency  $f$  in Hz corresponding to (a) Fig. 1 and (b) Fig. 2.

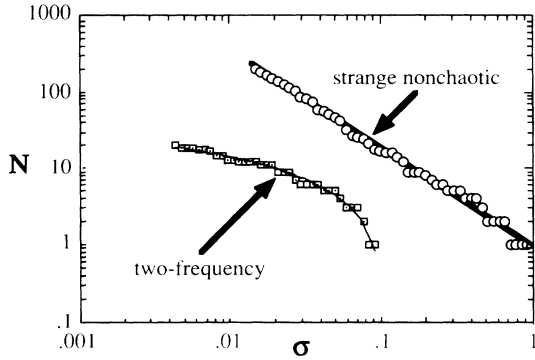


FIG. 4. Spectral distributions of the spectra of Figs. 3(a) and 3(b). The  $N(\sigma)$  spectrum for the strange nonchaotic case has only been plotted for  $\sigma \geq 0.01$  to avoid saturation of  $N(\sigma)$  due to the base line of  $|S(f)|$  at  $|S(f)| \sim 0.01$ . This saturation presumably occurs from the width acquired by  $\delta$ -function spectral components contributed either by noise broadening of the synthesized frequencies  $f_1$  and  $f_2$  or by the finite length of the time series.

tra of the two time series corresponding, respectively, to the surfaces of section of Fig. 1 and Fig. 2. Figure 3(a) shows the spectrum of the two-frequency quasiperiodic attractor to be concentrated on a discrete set of frequencies, while the spectrum shown in Fig. 3(b) exhibits a richer harmonic structure and notably higher base line.

Figure 4 displays the spectral distribution function  $N(\sigma)$  for the two spectra shown in Figs. 3(a) and 3(b). The spectrum in Fig. 3(a) exhibits the scaling  $N(\sigma) \sim \ln(\sigma)$ . In contrast, the spectrum of Fig. 3(b) exhibits the scaling  $N(\sigma) \sim \sigma^{-\alpha}$  with the best fit<sup>14</sup> giving  $\alpha = 1.25 (\pm 0.05)$ . These results are in agreement with the theoretical predictions given in Refs. 2 and 3. The spectra shown were calculated using a Parzen window (cf. Ref. 2); however, we found  $N(\sigma)$  to be unaffected by the particular choice of window function. A forthcoming simplified model for the ribbon in the form of a double-well Duffing equation with parametric quasiperiodic driving terms also displays spectral-distribution scaling in qualitative agreement with these results.<sup>15</sup>

Information-dimension calculations<sup>10</sup> have been performed for the attractors presented in Figs. 1 and 2. In each case a maximum of  $1000 \times 1000$  equally sized grid boxes were used to cover the attractor. The plot of  $I(\epsilon)$  vs  $\ln(1/\epsilon)$  for Fig. 2 is shown in Fig. 5. The slope is an estimate of the information dimension  $\tilde{d}_i$ . A least-squares fit to the data yields  $\tilde{d}_i \cong 1.3$  [excluding the region beyond  $\ln(1/\epsilon) > 5.5$ , whose values are less reliable due to the finite length of the time series].<sup>16</sup> The relevant point is that  $\tilde{d}_i$  is clearly well below 2. Thus we conclude that the attractor is nonchaotic.<sup>5</sup> (Similar results are obtained from the simplified model of the ribbon in Ref. 15.)

In order to obtain a feel for the dynamics on the strange nonchaotic attractor, we have examined the be-

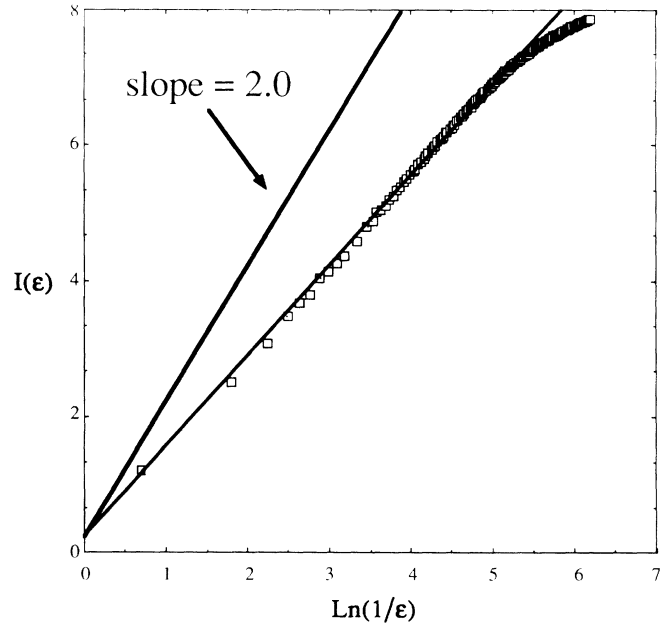


FIG. 5. Plot of  $I(\epsilon)$  vs  $\ln(1/\epsilon)$  for the strange nonchaotic attractor (using all 5000 data points).

havior of the separation between two nearby points of Fig. 2. We take our data string  $(V_n, \theta_n)$ , where  $\theta_n \equiv (nf_2/f_1) \pmod{1}$ , and choose two points,  $(V_j, \theta_j)$  and  $(V_{j'}, \theta_{j'})$ , such that  $|\theta_{j'} - \theta_j|$  is small. We then plot the difference in the vertical coordinate  $\delta_m \equiv |V_{j'+m} - V_{j+m}|$  vs  $m$  in Fig. 6 (note that  $|\theta_{j'+m} - \theta_{j+m}|$  does not vary with  $m$ ). We see from Fig. 6 that  $\delta_m$  displays a characteristic behavior wherein it is small for long stretches of time, increases to a large value for a very short time, and rapidly returns to small values. This is fundamentally different from what one sees for a chaotic attractor (wherein nearby points move exponentially apart and then execute motion that is essentially uncorrelated, e.g., Ref. 15; close returns are far less probable for this case). The behavior observed in Fig. 6 is indicative of the structure of the strange nonchaotic attractors observed in Refs. 1-5, where it was shown that these attractors are everywhere discontinuous *functions* of the horizontal coordinate [i.e., in our case  $V = F(\theta)$  where  $F(\theta)$  is discontinuous].

Finally, we note that strange nonchaotic attractors, similar to that in Fig. 2, were observed throughout the interval  $0.75 \text{ Oe} < H_2 < 0.90 \text{ Oe}$ , thus verifying their predicted existence over a set of positive measure in parameter space.<sup>1-5</sup>

In conclusion, the surface-of-section plots, scaling of the spectral distribution function, and information-dimension measurements provide compelling evidence that we have observed a strange nonchaotic attractor in a quasiperiodically driven magnetoelastic ribbon experiment. Future work will address the mechanism by which

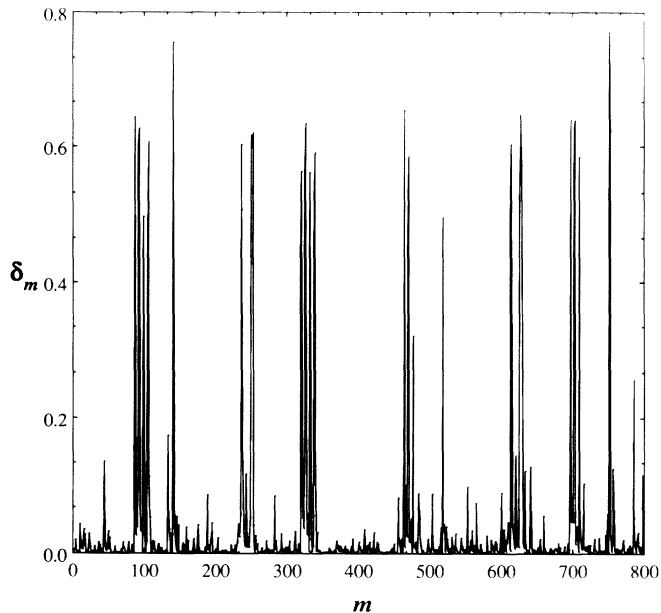


FIG. 6. Plot of  $\delta_m \equiv |V_{j+m} - V_{j+m}|$  vs  $m$  (voltages  $V_n$  have been scaled to the interval  $[0,1]$ ).

this transition occurs.

This work was supported by the Navy Dynamics Institute Program, the Naval Surface Warfare Center IR Program, and ONR. J.H. was supported through the Office of Naval Technology Postdoctoral Fellowship Program.

<sup>(a)</sup>Permanent address: University of Maryland, College Park, MD 20742.

<sup>1</sup>C. Grebogi, E. Ott, S. Pelikan, and J. A. Yorke, *Physica* (Amsterdam) **13D**, 261 (1985).

<sup>2</sup>A. Bondeson, E. Ott, and T. M. Antonsen, *Phys. Rev. Lett.* **55**, 2103 (1985).

<sup>3</sup>F. J. Romeiras, A. Bondeson, E. Ott, T. M. Antonsen, and C. Grebogi, *Physica* (Amsterdam) **26D**, 277 (1987).

<sup>4</sup>M. Ding, C. Grebogi, and E. Ott, *Phys. Rev. A* **39**, 2593 (1989); F. J. Romeiras and E. Ott, *Phys. Rev. A* **35**, 4404 (1987).

<sup>5</sup>M. Ding, C. Grebogi, and E. Ott, *Phys. Lett. A* **137**, 167 (1989).

<sup>6</sup>D.-R. He, W. J. Yeh, and Y. H. Kao, *Phys. Rev. B* **30**, 172 (1984).

<sup>7</sup>F. C. Moon and W. T. Holmes, *Phys. Lett. A* **111**, 157 (1985).

<sup>8</sup>G. A. Held and C. Jeffries, *Phys. Rev. Lett.* **56**, 1183 (1986).

<sup>9</sup>A. Wolf, J. B. Swift, H. L. Swinney, and J. A. Vasano, *Physica* (Amsterdam) **16D**, 285 (1985); J.-P. Eckmann and D. Ruelle, *Rev. Mod. Phys.* **57**, 617 (1985); M. Sano and Y. Sawada, *Phys. Rev. Lett.* **55**, 1082 (1985).

<sup>10</sup>J. D. Farmer, E. Ott, and J. Yorke, *Physica* (Amsterdam) **7D**, 153 (1983).

<sup>11</sup>J. Kaplan and J. A. Yorke, in *Functional Differential Equations and Approximation of Fixed Points*, edited by H.-O. Peitgen *et al.*, Springer Lecture Notes in Mathematics Vol. 730 (Springer-Verlag, Berlin, 1979), p. 228.

<sup>12</sup>W. L. Ditto, S. Raueo, R. Cawley, C. Grebogi, G.-H. Hsu, E. Kostelich, E. Ott, H. T. Savage, R. Segnan, M. L. Spano, and J. A. Yorke, *Phys. Rev. Lett.* **63**, 923 (1989).

<sup>13</sup>H. T. Savage and C. Adler, *J. Magn. Magn. Mater.* **58**, 320 (1986); H. T. Savage and M. L. Spano, *J. Appl. Phys.* **53**, 8002 (1982); H. T. Savage, W. L. Ditto, P. A. Braza, M. L. Spano, S. N. Raueo, and W. C. Spring, III, *J. Appl. Phys.* **67**, 5619 (1990).

<sup>14</sup>Attempting to fit the data with the "wrong" form [e.g., finite  $N(\sigma)$  arising from the quasiperiodic data with  $\sigma^{-\alpha}$ , or  $N(\sigma)$  from the strange nonchaotic data with  $\ln(\sigma)$ ] gives a  $\chi^2$  7 to 10 times larger than using the "correct" forms.

<sup>15</sup>W. L. Ditto and J. Heagy (to be published).

<sup>16</sup>Both our numerical work (Ref. 15) and that of Ding, Grebogi, and Ott (Ref. 5) indicate that  $\tilde{d}_i$  decreases slowly with successively larger data sets. Ding, Grebogi, and Ott indicate that prohibitively large data sets ( $> 10^9$  points) may be necessary to obtain values of  $\tilde{d}_i$  approaching 1.